A Molecularly Imprinted Polymer Nanoparticle Based Surface Plasmon Resonance Sensor Platform for Antibiotic Detection in River Water and Milk

Mark V. Sullivan[1], Alisha Henderson[1], Rachel A. Hand[1,2], Nicholas W. Turner[1]

Leicester School of Pharmacy, De Montfort University, The Gateway, Leicester, LE1 9BH, United Kingdom.

Department of Chemistry, Library Road, University of Warwick, Coventry, CV4 &AL, United Kingdom

Corresponding Email: nicholas.turner@dmu.ac.uk

Abstract

Using a solid-phase molecular imprinting technique, high affinity nanoparticles (nanoMIPs) selective for the target antibiotics, ciprofloxacin, moxifloxacin and ofloxacin have been synthesised. These have been applied in the development of a surface plasmon resonance (SPR) sensor for the detection of the three antibiotics in both river water and milk. The particles produced demonstrated good uniformity with approximate sizes of 65.8 ± 1.8 nm, 76.3 ± 4.1 nm and 85.7 ± 2.5 nm, and were demonstrated to have affinities of 36.2 nM, 54.7 nM and 34.6 nM for the ciprofloxacin, moxifloxacin and ofloxacin nanoMIPs, respectively. Cross reactivity studies highlighted good selectivity towards the target antibiotic compared with a non-target antibiotic. Using spiked milk and river water samples the nanoMIP-based SPR sensor offered comparable affinity with 66.8 nM, 33.4 nM and 55.0 nM (milk) and 39.3 nM, 26.1 nM and 42.7 nM (river water) for ciprofloxacin, moxifloxacin and ofloxacin nanoMIPs respectively, to that seen within a buffer standard. Estimated LOD's for the three antibiotic targets in both milk and river water were low nM or below. The developed SPR sensor showed good potential for using the technology for the capture and detection of antibiotics from food and environmental samples.

Keywords:

Molecularly Imprinted Polymer, Antibiotic, Surface Plasmon Resonance, Fluoroquinolone, River water, Milk

Introduction

Antibiotics are undoubtedly one of the most successful pharmaceutical classes in the history of medicine. They are used in the fight against bacterial infections, with antibiotic medications being widely used in the treatment and prevention of bacterial infections (1). While the use of antibiotics can be dated back to ancient times, it wasn't until the 20th Century that their use became widespread and proved to be significantly valuable during wartime (2, 3). Antibiotics are primarily classified based on their spectrum of activity, chemical structure or mechanism of action; with most antibiotics targeting bacterial functions or growth process (2, 3). Fluoroquinolones are a commonly prescribed class of antibiotics that are, due to their dose simplicity and effectiveness, widely prescribed for a range of ailments including, pneumonia, as well as skin and abdominal infections (4). Ciprofloxacin, moxifloxacin and ofloxacin are common and popular examples of this family (Figure 1).

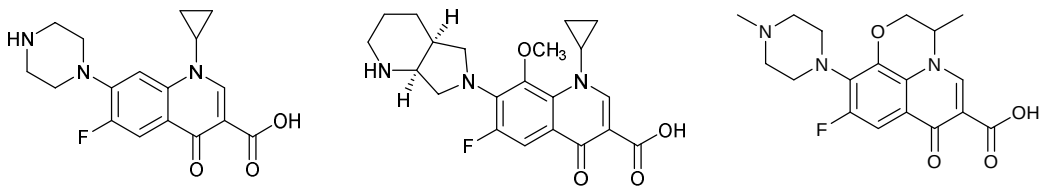

Figure 1: Structures of ciprofloxacin (left), moxifloxacin (centre) and ofloxacin (right). The presence of the fluorine at C6 highlights the distinguishing factor of this class over the first-generation quinolone compounds.

Due to their effectiveness, and ubiquity, their widespread use has become a cause for concern (4). The overuse of fluoroquinolones has demonstrably increased the spread of antibiotic resistance and this is widely recognised as a major global problem that needs addressing (5). This rapid spread of antibiotic resistance in the food chain is increasing the risk of transmission of resistant bacteria of animal origin to humans, posing a serious threat to health. Furthermore, the widespread prospective use of fluoroquinolones in animal agriculture, is leading to drug residues accumulating through the food chain, and in the water supply (6), leading to imposed maximum residue limits (MRLs) for food of animal origin, with levels in environmental samples varying in the ppb-ppm range, depending on the molecule and matrix (7) across numerous countries. Consequently, from an analyst point-of-view, there is an important need to be able to accurately quantify trace amounts of antibiotics from within complex matrices.

Biological recognition molecules, such as antibodies and enzymes, are well known for their use in analytics and diagnostics, due to their strong affinities and specificity (8). When used in biosensors, these recognition molecules have been incorporated into a vast range of analytical methodologies and offer sensitive levels of detection (8). However, with limited reusability, these recognition molecules have some downsides. They are viewed as expensive and time-consuming to produce; exhibit batch-to-batch variations; process stability; while their performance can be affected by changes in pH, temperature, ionic strength with environmental degradation a significant problem (9, 10). This has resulted in research being directed towards synthetic recognition molecules as suitable alternatives, especially in applications (food/environmental) where robustness is an important factor.

Molecularly imprinted polymers (MIPs) are synthetic recognition materials that have gained interest (in both academic and commercial applications) due to their potential to match biological-based recognition molecules in performance, while countering a number of the downsides (11). MIPs have consistently demonstrated their robustness in a variety of conditions (12, 13). The principle is relatively simple to envisage. Functional monomers form a complex around a template (the target analyte) via non-covalent interactions. This complex is entrapped by polymerisation into a highly cross-linked polymer structure. After the removal of the template, the polymer bears binding cavities that are sterically and functionally complimentary to the template molecule, (12, 14). The development and enhancement of MIP nanoparticles (nanoMIPs – imprinted materials < 200 nm diameter) has significantly improved performance of MIPs by reducing binding site heterogeneity, while increasing potential scope within biological systems, not just within sensors (15, 16), leading to a flexibility in use (17). The small particulate size of nanoMIPs allows for more regular structures with a high surface area to volume ratio, and a greater yield of useable product which is in contrast to the more traditional bulk MIP, (18). NanoMIPs have the ability to offer excellent binding capacities and performances that is comparable to that of natural counterparts (antibodies) (19). The synthetic method for these materials also led to observed one binding site per nanoparticle, allowing them to be easily modelled with mathematical functions commonly employed for biological recognition elements.

Antibiotics have long been a target for MIP development with mixed success (20-22). In example, Jameson *et al.* using a screen-printed electrode, successfully utilized MIPs as synthetic receptors for the detection of Amoxicillin. Producing a low-cost sensor platform, using a direct polymerisation technique, the sensor was able to achieve a limit of detection (LOD) of 0.54 nM (23). By incorporating a fluorescent monomer (fluorescein methacrylate) into a MIP film allowed Hudson *et al.* to produce a sensor that was capable of detecting nafcillin, offering the potential for a portable, on-site sensor (24). MIPs have shown demonstrable application in solid phase extraction protocols and a range of fluoroquinolones have been targeted from environmental and animal product samples (25-27). This can be linked to high-end analytical tools such mass spectrometry (25-27).

Surface Plasma Resonance (SPR) is commonly used optical sensor platform with a high degree of sensitivity (28). SPR-based biosensors have been used since the 1980s, where they have been

successfully used in a range of fields, and both antibodies and enzymes are commonly used recognition materials (28, 29). There have been several attempts to incorporate MIPs as the synthetic receptors for the recognition element in SPR analysis, either by thermal polymerization or photoinitiated polymerization to deposit an imprinted layer, (30, 31); or by using an EDC/NHS coupling method has allowed for nanoMIPS to be immobilised onto the surface of a gold SPR chip bearing carboxyl groups (32). Due to its exceptional sensitivity, SPR has become ubiquitous in sensor development due to the ease of analysis and robust nature of the technology.

Recently our group used Moxifloxacin as a template in the development of aptamer-bearing MIPs (18), studied by SPR. These "aptaMIPs" utilise a prior selected aptamer sequence as a "macromonomer" to increase the affinity of the binding pocket. The focus of this prior study was not only to demonstrate the aptaMIP technique on a relevant small bioactive target, but also to highlight a different functionality for aptamer incorporation. In the case of moxifloxacin, the aptaMIP had approximately a 10-fold improvement in dissociation constant over a plain nanoMIP (K_D values of 3.65 × ± 0.9 nM, and 48.60 ± 7.0 nM for the aptaMIP and nanoMIP respectively. This ability to maximise the affinity is vital when targeting certain compounds (those of high value, or scarcity), or when the sensor is bespoke and ultimate performance is required; however, the use of an aptamer macromonomer brings added complexity in the synthetic route and increased cost (SELEX development and aptamer synthesis), and as such it is not always wanted or needed. It is important to recognise that for some applications cost is a significant factor, and that K_D's in the range 10^{-8} are sufficient to task. In environmental sampling, where ideally numerous sensors would be deployed, the synthesis of a recognition element needs to be cost effective and subject to simple manufacture processes. It is in this light, that we present this study. Here we develop high performance nanoMIPs for the recognition and detection of three target antibiotics, Ciprofloxacin, Moxifloxacin and Ofloxacin and tested their efficacy in a sensor platform.

The nanoMIPs were synthesized using a recently established solid-phase approach (15) and analysed using the SPR. Once polymer performance was understood, the sensor was exposed to spiked milk and river water samples to show the effectiveness of a nanoMIP-based SPR sensor within relevant biological matrices.

Experimental

Materials

Acrylic acid (AA), 3-aminopropyltrimethyloxy-silane (APTMS), ammonium persulfate (APS), ciprofloxacin, 1-Ethyl-3-(3-dimethylaminopropyl)carbodiimide (EDC), glutaraldehyde (GA), glycine, moxifloxacin, N-(3-aminopropyl)methacrylamide hydrochloride (NAPA), *N,N*'-methylenebisacrylamide (BIS), *N*-hydroxysuccinimide (NHS), *N*-isopropylacrylamide (NIPAm), ofloxacin, sodium dodecyl sulphate (SDS), *N*-*tert*-butylacrylamide (TBAm), and tetramethylethyldiamide (TEMED), were all purchased from Sigma-Aldrich (Poole, Dorset, UK).

Acetone, acetonitrile (dry), dipotassium phosphate, disodium phosphate, ethanolamine, ethylenediaminetetraacetic acid (EDTA), methanol, potassium chloride, sodium hydroxide and Tween 20 were all purchased from Fisher Scientific UK (Loughborough, Leicester, UK).

Glass beads (75 µm diameter) were purchased from Microbeads AG, (Brugg, Switzerland) and used as found.

All chemicals and solvents were analytical quality or high-performance liquid chromatography (HPLC) grade and were used as found without further purification.

Skimmed Milk was purchased from Tesco Ltd and used fresh, while the river water was collected from the River Soar on the 5th August 2021 at co-ordinates 52°37'51.2"N 1°08'32.7"W.

Methods

Preparation of Antibiotic-Derivatized Glass Beads as Affinity Media

The preparation of the glass beads was as described in our prior work (18). Before template attachment, these were activated by boiling in 4 M NaOH (24 mL) for fifteen minutes, washed with reverse-osmosis water (8 x 100 mL for 30 g of beads), until the resultant solution was pH 7. They were then subjected to 100 mL acetone wash and dried at 80 °C for three hours.

The beads were placed into 12 mL solution of APTMS (3%, v/v) in anhydrous toluene overnight at 60 °C, then further washed (8 x 100 mL acetone; (2 x 100 mL methanol). Finally, after draining, the beads were placed into an oven (150 °C for 30 minutes). These beads can be stored, in inert, dry, cool conditions for one month but ideally should be used straight away.

The template antibiotic (ciprofloxacin, moxifloxacin or ofloxacin) (9 mg of compound dissolved in 15 mL of phosphate-buffered saline (PBS, 10 mM, pH 7.4). To this mixture, 600 mg of EDC and 150 mg of NHS were dissolved. The solution was purged using a nitrogen stream for 15 minutes, and then added to the functionalized beads and left under nitrogen at room temperature (RT) for 15 hours. The mixture was agitated slightly using a slow rocker (fast agitation such as stirring risks abrading the beads). After this incubation, the beads were washed thoroughly (8 x 100 mL water) and dried under vacuum at room temperature. When dry, the template functionalised beads were used immediately.

Solid-Phase Synthesis of Moxifloxacin Imprinted nanoMIPs

Synthesis of the nanoMIPs was performed using a well-developed and widely accepted solid-phase method (15, 16), (18), scaled to 30g of beads.

In summary a 50 mL aqueous solution bearing 2.2 µL AA, 1 mg BIS, 7 mg NAPA, 20 mg NIPAm, and 10 mg TBAm (dissolved prior in 250 µl ethanol) was generated. This was degassed sonicating under vacuum (10 minutes), then sparged with N_2 (20 minutes).

The 30g of bead were placed in a 100 mL sealable Duran bottle which was and purged with N_2 (10 minutes) before the addition of the polymerisation solution. To this mixture 12.5 µL TEMED and 15 mg APS dissolved in 250 µL were added to start the polymerisation reaction. Th reaction was left on a slow swirl rocker for 1 hour at RT.

To stop the reaction, the beads were gravity filtered through 11 µm paper, and *in-situ* washed (8 x 30 mL water) at RT to removed unwanted materials and unused reactants. This step also washes off low-affinity nanoMIPs (15, 16). The beads were then collected and heated to 60 °C in 40mL water then filtered through 11 µm paper with the filtrate collected. A series of water washes at 60 °C were carried out until approximately 100 mL of eluted high-affinity nanoparticles was collected. This solution was allowed to cool to ambient temperature naturally, then stored at 4 °C.

Characterization of Nanoparticles

A 3 mL aliquot of the solution was oven-dried at 60 °C and the mass of the particles measured using a 6-point balance, allowing for a concentration (in µg mL^{-1}) of the initial solution to be calculated. Particle size at 25 °C (effective hydrodynamic diameters (d_h) was measured using dynamic light scattering in PBST (Brookhaven NanoBrook Omni spectrometer using *Particle Solutions* v 2.6) with n=5.

Affinity and specificity of the imprinted nanoparticles for the different targets were studied using a Reichert 2 SPR system (Reichert Technologies, Buffalo, USA) with attached autosampler.

Immobilisation of nanoMIPs onto the SPR Sensor Surface

A carboxymethyl dextran hydrogel coated Au chip was preconditioned by a PBS pH 7.4 and 0.01 % Tween 20 running buffer (referred as PBST) at 10 µL min^{-1} within the SPR. 1 mL of aqueous solution containing 40 mg EDC and 10 mg NHS was passed over the chip (6 minutes at 10 µL min^{-1}).

300 µg of nanoMIPs in 1 mL of PBST and 10 mM sodium acetate, was injected over the left channel (working channel) of the chip for 1 minute. The amine groups on the nanoMIP react with the functionalised surface leading to particle immobilisation. An 8-minute injection over both channels (working and reference) of quenching solution (1 M ethanolamine, pH 8.5) was added; followed by a continuous flow of PBST at 10 µL min^{-1} All injections were taken from a stable baseline.

Kinetic Analysis Using SPR

Kinetic analysis in rebinding of analyte (target and cross-reactivity) to the nanoMIP was performed in set pattern of 2-minute association (PBST with analyte in range of 1.95 – 31.25 nM), 5-minute dissociation (PBST only) and a regeneration cycle (regeneration buffer 10 mM Glycine-HCl, pH 2 for 1 minute) followed by a final stabilisation cycle (PBST for 1 minute). An initial injection of blank PBST was used as the first run with increasing analyte concentration for subsequent runs. After the analyses were completed, signals from reference channel were subtracted from signals from the working. In all cases rebinding was studied in triplicate.

The SPR responses were fitted to a 1:1 Langmuir git bio-interaction (BI) model using the Reichert *TraceDrawer* software. Association rate constants (k_a), dissociation rate constants (k_d), and maximum binding (B_{max}) were fitted globally, whereas the BI signal was fitted locally. Equilibrium dissociation constants (K_D) were calculated by k_d/k_a.

For each nanoMIP/analyte combination, a calibration curve was generated across the concentration range 1.95-31.25 nM taking n=3 average. From this a theoretical limit of detection (LOD) was calculated. Where signal saturation was observed (noted in more complex matrices), the linear section of the curve was used for this calculation.

Results and Discussion

Using the prior work of Poma et al. (15) the composition and reaction conditions for imprinted nanoparticles was selected (33). We adapted the work of Canfarotta *et al*, where nanoMIPs were successfully synthesised for template molecules that contain -COOH functional groups of similar size to the antibiotic used in this study (16). This was logical as all three compounds bear this functionality, at one end of the molecule. Three different novel molecularly imprinted polymer nanoparticles (nanoMIPs) were produced for the target antibiotics ciprofloxacin, moxifloxacin and ofloxacin. Due to the thermoresponsive properties (incorporation of NIPAm that gives the material thermal flexibility within the cross-linked matrix) of the nanoMIPs, they are easily removed from the solid support during the synthetic step, without the any conservation of the site structure being lost (15)(34, 35).

The concentrations of the ciprofloxacin, moxifloxacin or ofloxacin nanoMIP solutions after synthesis were calculated to be 54.3 ± 2.3 µg mL^{-1}, 44.6 ± 3.1 µg mL^{-1} and 64.6 ± 2.3 µg mL^{-1}, respectively. In total approximately 100 mL of the nanoparticle solution is synthesised, suggesting our overall yield for a single synthesis is between 4.4 and 6.4 mg of nanoparticles. Given that we use 300 µg per chip preparation, this yield is more than adequate for our studies, including repeats.

The nanoMIPs were then analysed by DLS (Figure S1), with the diameters of the particles being 65.8 ± 1.8 nm, 76.3 ± 4.1 nm and 85.7 ± 2.5 nm at 25 °C, for ciprofloxacin (Figure S1A), moxifloxacin (Figure S1B) for ofloxacin (Figure S1C), respectively. The curves produced by DLS (Figure S1) show good Gaussian distributions, though there is slight difference between target specific materials in terms of polydispersity. These values are consistent with prior literature where uniformity in size and shape has been shown (32, 36, 37).

Binding performance of small molecules to synthesised imprinted nanoparticles.

The amine functionality on the nanoMIP polymer scaffold will readily react (these are abundant due to the monomer composition), allowing for a coupling reaction, covalently linking the particle to the surface of the SPR chip. A solution of ethanolamine is finally used to deactivate any unreacted carboxyl groups on the chip surface and wash away any unbound nanoMIPs. The nanoMIP modified surfaces were then used for affinity studies, and to generate a calibration curve/theoretical detection limit for each compound within the different matrices.

Due to the EDC/NHS coupling chemistry used in the immobilisation of the amine functionalised nanoMIPs to the SPR chip surface, a monolayer of the nanoMIPs is expected to be deposited on the surface, as the polymers will bind only to the surface, and not to themselves Adding the initial deposition of nanoMIPs in excess, in a relatively slow flow, achieves maximal coverage on the chip. A schematical representation of how the nanoMIP covalently binds to the carboxymethyl dextran hydrogel SPR chips is shown in Figure S2. Given the size and nature of the nanoMIPs, this allows standard biological kinetics methods for analysing the binding of a ligand to a receptor, using a 1:1 kinetics model to be applied.

Figure 2 shows the interactions of the target molecules at five different concentrations with ciprofloxacin nanoMIP (Figure 2A), moxifloxacin nanoMIP (Figure 2B) and ofloxacin nanoMIP (Figure 2C), immobilised on the sensor surface. The addition of 0.01% Tween20 to the running buffer enables the reduction of non-specific binding (18, 19). An example of the fitted curves (Figure 2) matched with their raw data is shown in Figure S3A (ciprofloxacin nanoMIP), Figure S3B (moxifloxacin nanoMIP, and Figure S3C (ofloxacin nanoMIP), respectively.

To study cross-reactivity and non-specific binding, the two non-target antibiotics were also introduced the nanoMIP coated gold chip. Moxifloxacin and ofloxacin were used for the ciprofloxacin nanoMIP (Figure 2D and 2G, respectively); ciprofloxacin and ofloxacin for the moxifloxacin nanoMIP (Figure 2E and 2H, respectively); and lastly ciprofloxacin and moxifloxacin for the ofloxacin nanoMIP (Figure 2F and 2I, respectively). The SPR curves being fitted to a 1:1 interaction model. The overall equilibrium dissociation constants (K_D) of each target specific nanoMIP towards the target and non-target antibiotics were determined from average of at least three replicates, and summarised in Table 1. The association constant (K_a) and dissociation constants (K_d) used to calculate the equilibrium dissociation constant (K_D) alongside representative fitted curves are presented in the supplementary information (Figure S3 and Tables S1 and S2).

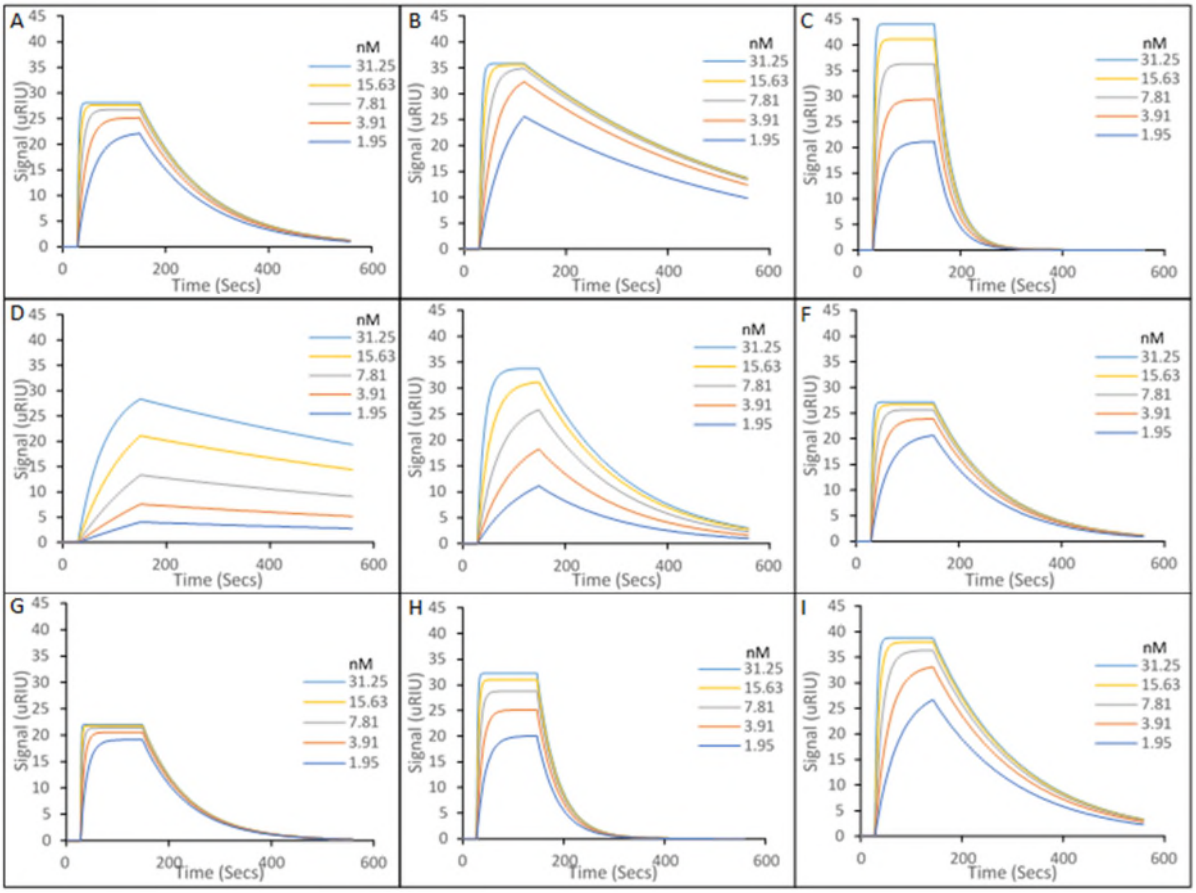

Figure 2. Representative sensorgrams of molecular interactions of different imprinted nanoMIPs immobilised onto a carboxymethyl dextran hydrogel coated gold SPR chips for five concentrations of antibiotic target and non-target molecule targets. The top row shows the response of specific nanoIP to its respective target: **(A)** ciprofloxacin binding to ciprofloxacin-imprinted nanoMIPs; **(B)** moxifloxacin binding to moxifloxacin-imprinted nanoMIPs; and **(C)** ofloxacin binding to oxfloxacin-imprinted nanoMIPs. The centre and bottom rows show cross-reactivity binding of nanoMIP to alternative familial compounds, highlighting the selectivity of the generated imprints: **(D)** moxifloxacin binding to ciprofloxacin-imprinted nanoMIPs; **(E)** ciprofloxacin binding to moxifloxacin-imprinted nanoMIPs; **(F)** ciprofloxacin binding to ofloxacin-imprinted nanoMIPs; **(G)** ofloxacin binding to ciprofloxacin-imprinted nanoMIPs; **(H)** ofloxacin binding to moxifloxacin-imprinted nanoMIPs; and **(I)** moxifloxacin binding to ofloxacin-imprinted nanoMIPs.

The K_D of the interaction between the antibiotic target molecules and their corresponding nanoMIP materials have been calculated at 36.2 nM, 54.7 nM and 34.6 nM (Table 1) for ciprofloxacin, moxifloxacin and ofloxacin nanoMIPs, respectively as an average of triplicate runs. The K_D values obtain within this work are similar to that of the K_D values previously obtained for this type of small molecule imprinted nanoMIPs. Work by Caro et al. produced a nanoMIP for the antibiotic Florfenicol, that obtained a K_D value of 75 nM and in practical terms resembled monoclonal antibodies (38).

As seen in Figure 2, the generated materials were also assessed for their specificity towards their target molecules. As Table 1 shows, the nanoMIPs, when loaded with a non-target antibiotic, produce K_D values into the µM range, thus showing a 100-fold decrease in affinity and demonstrating target specificity, consistent with similarly produced nanoMIPs (37, 38). This is a significant demonstration of selectivity given the similarity in structure shown in Figure 1.

Table 1. Calculated equilibrium dissociation constant (K_D) of target specific nanoMIPs against varied analytes. All experiments performed under ambient conditions. Number of repeats =3

	K_D (M)		
	Ciprofloxacin	Moxifloxacin	Ofloxacin
Ciprofloxacin nanoMIP	3.62×10^{-8} ($\pm 0.26 \times 10^{-8}$)	1.78×10^{-6} ($\pm 0.27 \times 10^{-6}$)	1.48×10^{-6} ($\pm 0.25 \times 10^{-6}$)
Moxifloxacin nanoMIP	6.60×10^{-6} ($\pm 0.32 \times 10^{-6}$)	5.47×10^{-8} ($\pm 0.34 \times 10^{-8}$)	1.35×10^{-6} ($\pm 0.20 \times 10^{-6}$)
Ofloxacin nanoMIP	6.60×10^{-6} ($\pm 0.43 \times 10^{-6}$)	1.67×10^{-6} ($\pm 0.26 \times 10^{-6}$)	3.46×10^{-8} ($\pm 0.32 \times 10^{-8}$)

Fluoroquinolones, such as the template molecules used, are commonly used in veterinary treatment of bacterial infections in dairy production, and are known to be transferred to milk and there is a concern that the presence of antibiotic residues in foods of animal origin, like dairy and milk, can further the spread of antibiotic-resistant bacterial strains (39). Some fluoroquinolones, like enrofloxacin, can metabolise into other active fluoroquinolones (ciprofloxacin), which can then be found in the milk of the animals (40). This means antibiotic residues in animal origin foods are closely monitored and established maximum residue limits (MRL) are set to levels recognized as acceptable in food (41).

Likewise, excess use of stable antibiotics in husbandry can lead to runoff (from urine and food waste) into river systems, alongside leaks from waste water treatment, or manufacturing sites (42-44). Thus, being able to detect antibiotics in foods of animal origin (milk) and environmental samples is important, especially in the monitoring and prevention of antibiotic resistance. A single sensor capable of doing both would be a powerful tool.

Figure 3 shows the SPR sensorgrams for the interactions of milk samples, spiked with the target antibiotics, and their corresponding nanoMIP SPR sensor chip, with Ciprofloxacin shown in Figure 3A, Moxifloxacin Figure 3B and Ofloxacin Figure 3C. Figures 3D, 3E and 3F show plotted concentration calibrations (Ciprofloxacin, Moxifloxacin, and Ofloxacin, respectively), allowing for the estimation of the theoretical LOD.

It should be noted that only the lower three concentrations (1.95, 3.91 and 7.81 nM) were used for the calibration plots, as it was only these concentrations that form the linear portion of the calibration. Above this the limit of linearity was reached and at higher concentrations, some saturation of signal was observed. The saturation can be seen in calculated signal in the SPR plots in Figures 2, 3 and 4. This was consistent across all replicates and all systems tested. The K_D values and estimated theoretical lower LOD for the detection of the target antibiotics from a milk sample, are summarized in Table 2. The association constant (K_a) and dissociation constants (K_d) used to calculate the equilibrium dissociation constant (K_D) are presented in the supplementary information (Tables S1 and S2).

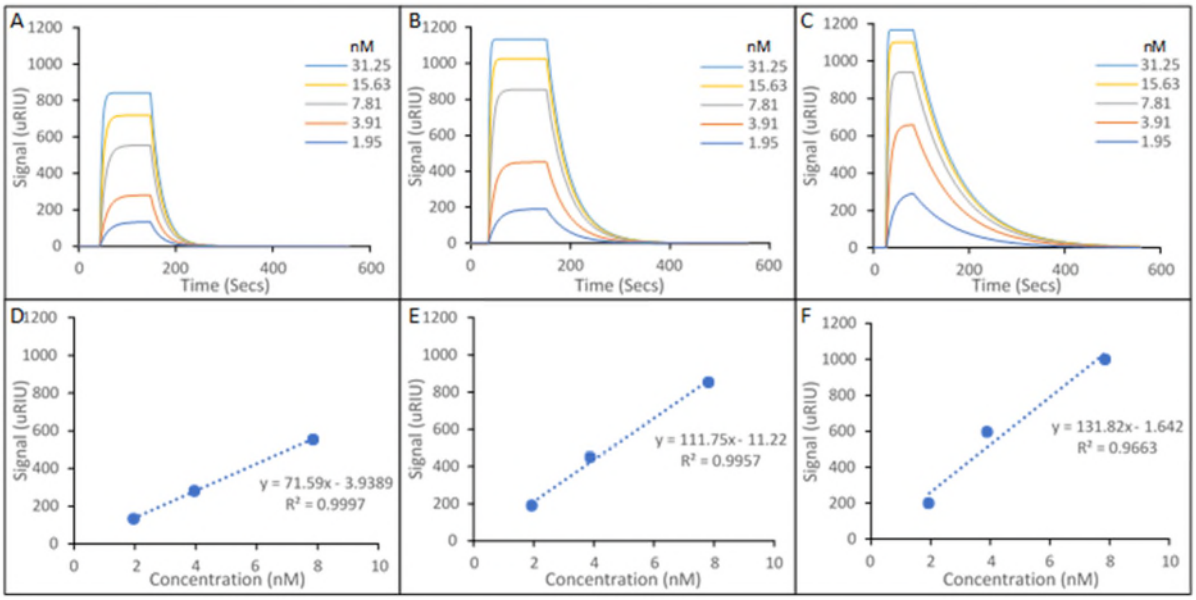

Figure 3. Representative sensorgrams of interactions of different imprinted nanoMIPs immobilised onto a carboxymethyl dextran hydrogel coated gold SPR chips for five concentrations of antibiotic target in spiked milk samples. **(A)** ciprofloxacin binding to ciprofloxacin-imprinted nanoMIPs; **(B)** moxifloxacin binding to moxifloxacin-imprinted nanoMIPs; and **(C)** ofloxacin binding to ofloxacin-imprinted nanoMIPs. Representative calibration curves showing relative signal vs concentration: **(D)** ciprofloxacin binding to ciprofloxacin-imprinted nanoMIPs concentration calibration; **(E)** moxifloxacin binding to moxifloxacin-imprinted nanoMIPs concentration calibration; and **(F)** ofloxacin binding to ofloxacin-imprinted nanoMIPs concentration calibration.

The sensorgrams shown in Figure 3 show in intensity signals, which are greatly increased, when compared to the sensorgrams shown in Figure 2. This is to be expected, as SPR uses changes in refractive index for measurement, (45) and milk will be significantly different to simple PBST buffer. The calculated K_D values, shown in Table 2, are consistent with those shown in Table 1, with 36.2 nM, 54.7 nM and 34.6 nM (Table 1) compared with 66.8 nM, 33.4 nM and 55.0 nM (Table 2) for ciprofloxacin, moxifloxacin and ofloxacin nanoMIPs, respectively. We would expect slightly different affinities based on the differences in the environment (pH, ionic strength, viscosity etc.) and this is also observed in the river water samples below.

This data shows that specific antibiotic detection is achievable in animal food product (milk) samples. The theoretical LOD limits calculated are 0.55 nM, 1.00 nM and 0.13 nM for ciprofloxacin, moxifloxacin and ofloxacin, respectively and show that these nanoMIPs have the ability to detect low concentrations of the target molecules. These LODs are superior to the detection of moxifloxacin by SPR, using a protein recognition agent (~5 nM) (46), as well being comparable to chemiluminescent techniques (0.5 nM) (47) and other antibiotic MIP-based sensors (0.51 nM) (48). This demonstrates that the LOD limits estimated are within the practical application range for the antibiotic detection in food animal product (milk).

Table 2. Calculated equilibrium dissociation constant (K_D) of imprinted materials with target reload from spike milk samples and estimated theoretical lower LOD. All experiments performed under ambient conditions. Number of repeats =3.

	(M)		
	Ciprofloxacin	Moxifloxacin	Ofloxacin

Target reloaded from spiked milk sample	6.68×10^{-8} ($\pm 0.16 \times 10^{-8}$)	3.34×10^{-8} ($\pm 0.12 \times 10^{-8}$)	5.50×10^{-8} ($\pm 0.23 \times 10^{-8}$)
Theoretical LOD of Target reloaded from spiked milk sample	5.50×10^{-10}	1.00×10^{-9}	1.25×10^{-10}

To further explore the practical applications of the nanoMIP sensor system, we repeated this study using river water, collected from the River Soar, Leicester, UK, spiked with the target antibiotics (Figure 4). Note that the water was filtered through a 0.22 µm filter to remove sediment and any organic matter (bacteria etc.). The SPR sensorgrams for the interactions of river water samples, spiked with the target antibiotics, and their corresponding nanoMIP SPR sensor chip, with ciprofloxacin shown in Figure 4A, moxifloxacin Figure 4B and ofloxacin Figure 4C. Figures 4D,4E and 4F show plotted concentration calibrations, allowing for the estimation of the theoretical LOD. Again, it should be noted that only the lower three concentrations (1.95, 3.91 and 7.81 nM) were used for the calibration plot, as it was only these concentrations that form the linear portion of the calibration. As discussed above with the milk there is a matrix effect in place that lead to consistent saturation of signal at higher concentrations. The K_D values and estimated theoretical lower LOD for the detection of the target antibiotics from a river water sample, is summarized in Table 3. The association constant (K_a) and dissociation constants (K_d) used to calculate the equilibrium dissociation constant (K_D) are presented in the supplementary information (Tables S1 and S2).

The sensorgrams shown in Figure 4 show in intensity signals, which are much reduced, when compared to the sensorgrams shown in Figure 3, but are still increased when compared those shown in Figure 2. Again, this is to be expected, as the river water sample is a less complex media, compared with milk, but will still contain contaminants and a different composition to buffer.

The calculated K_D values, shown in Table 3, are consistent with those shown in Table 1 and 2 (buffer and milk). These theoretical LOD limits calculated are 0.51 nM, 0.92 nM and 0.16 nM, for ciprofloxacin, moxifloxacin and ofloxacin nanoMIPs, respectively, are also consistent with those detected from the milk samples (Table 2), which are supported by literature (46-48), and further demonstrates that these LOD limits are within the practical application range for environmental samples. Combined, this shows that specific and low-level antibiotic detection is achievable in environmental (river water) samples.

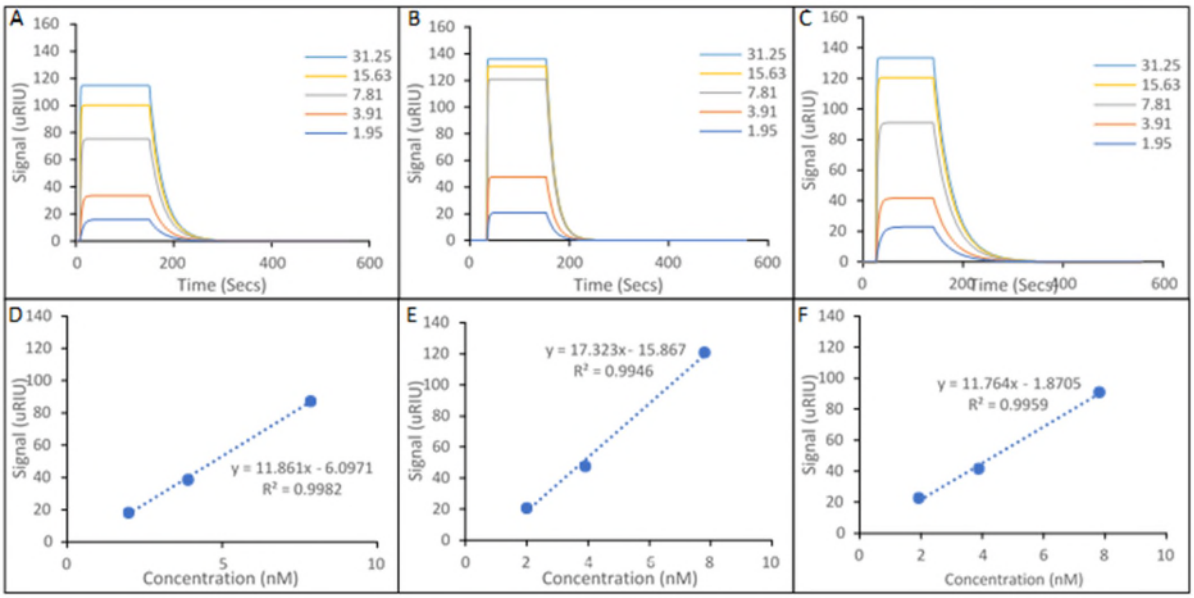

Figure 4. Representative sensorgrams of interactions of different imprinted nanoMIPs immobilised onto a carboxymethyl dextran hydrogel coated gold SPR chips for five concentrations of antibiotic target in spiked river water samples: **(A)** ciprofloxacin binding to ciprofloxacin-imprinted nanoMIPs; **(B)** moxifloxacin binding to moxifloxacin-imprinted nanoMIPs; and **(C)** ofloxacin binding to oxfloxacin-imprinted nanoMIPs. Representative calibration curves showing relative signal vs concentration: **(D)** ciprofloxacin binding to ciprofloxacin-imprinted nanoMIPs concentration calibration; **(E)** moxifloxacin binding to moxifloxacin-imprinted nanoMIPs concentration calibration; and **(F)** ofloxacin binding to oxfloxacin-imprinted nanoMIPs concentration calibration.

Table 3. Calculated equilibrium dissociation constant (K_D) of imprinted materials with target reload from spiked river water samples and estimated theoretical lower LOD. All experiments performed under ambient conditions. Number of repeats =3.

	(M)		
	Ciprofloxacin	Moxifloxacin	Ofloxacin
Target reloaded from spiked milk sample	3.93×10^{-8} ($\pm 0.28 \times 10^{-8}$)	2.61×10^{-8} ($\pm 0.19 \times 10^{-8}$)	4.27×10^{-8} ($\pm 0.38 \times 10^{-8}$)
Theoretical LOD of Target reloaded from spiked milk sample	5.14×10^{-10}	9.16×10^{-10}	1.59×10^{-10}

Conclusion

We have demonstrated the selective molecular recognition of a series of molecularly imprinted nanoparticles specific for three antibiotics ciprofloxacin, moxifloxacin and ofloxacin, using a solid-phase synthesis. This method produced nanoMIP particles with high affinity (K_D value of target in 10^{-8} M range) and high selectivity (K_D value of non-target analyte in 10^{-6} M range) observed being consistent with previous studies as well as being equivalent to monoclonal antibodies. The quality and

size of the produced nanoMIPs were characterised prior to the surface plasmon resonance based optical sensor affinity testing, with the size of the nanoMIPs found to be suitably uniform.

By immobilising these nanoMIPs on a SPR sensor platform, an effective stable method for detecting low concentrations of the targets in complex and commercially important matrices has been demonstrated, with theoretical LODs in the nM range, which is environmentally relevant. The performance in terms of levels of detection are also comparable to the detection levels in buffer calculated in our prior aptaMIP study (18). This highlights the strength of the imprinting process and that while it is correct to chase even greater affinity for certain targets/applications, often maximal performance is not required. A suitable analogy would be that of monoclonal and polyclonal antibodies, both of which have viable applications, despite different performance profiles.

This work also highlights that reported equilibrium dissociation constants, and LODs may differ between matrices. This is vital when presenting data for sensor systems or other applications of these materials, and we encourage our peers to further consider matrix effects. We intend to look to study this on this, and similar systems.

The current system highlights the power of SPR, but at the moment only offers a single compound detection. NanoMIPs are incredibly flexible materials and we are exploring incorporation of these into systems, including electrochemical platforms. Our current studies involve exploring these three compound-specific nanoMIPs, alongside others synthesised for other antibiotics within a multiplex electrochemical device to enable familial detection. This would bring the power of these robust, cost-effective recognition elements into practical applications.

This work also offers some questions in the synthetic methods. There is a slight, but noticeable difference in the size and polydispersity of the nanoMIPs when introduced to similar sized targets. This phenomenon has been observed in other studies (16-19). While the materials produced are practicable, and that the synthesis is standardised between sample, we believe that this should be studied. We hypothesise that this may be related to the nature/strength of the monomer/template complex, and its role in initial nucleation. A separate study on this is underway.

Acknowledgements

MS and NT would like to thank EPSRC for financial support for this work (EP/S003339/1). AH wishes to thank Professor Anwar Baydoun and the Faculty of Health & Life Sciences graduate program for financial support.

Declarations

The authors have no competing interests to declare.

References

1. Nicolaou KC, Rigol S. A brief history of antibiotics and select advances in their synthesis. J. Antibiot. 2018;71(2):153-84.

2. Laskin AI, Bennett JW, Gadd GM. Advances in Applied Microbiology. 1st Ed. ed. Amsterdam: Academic Press; 2003.

3. Clardy J, Fischbach MA, Currie CR. The natural history of antibiotics. Curr. Biol. 2009;19(11):R437-41.

4. Kabbani S, Hersh AL, Shapiro DJ, Fleming-Dutra KE, Pavia AT, Hicks LA. Opportunities to improve fluoroquinolone prescribing in the united states for adult ambulatory care visits. Clin. Infect. Dis. 2018;67(1):134-6.

5. Redgrave LS, Sutton SB, Webber MA, Piddock LJV. Fluoroquinolone resistance: Mechanisms, impact on bacteria, and role in evolutionary success. Trends Microbiol. 2014;22(8):438-45.

6. Brown SA. Fluoroquinolones in animal health. J. Vet Pharmacol. Ther. 1996;19(1):1-14

7. Ventola CL. The antibiotic resistance crisis: Part 1: Causes and threats. Pharm. Ther. (P&T). 2015;40(4):277-83.

8. Morales MA, Halpern JM. Guide to selecting a biorecognition element for biosensors. Bioconjug. Chem. 2018;29(10):3231-9.

9. Sharma PS, Iskiero Z, Pietryzyk-Le A, D'Souza F, Kutner W. Bioinspired intelligent molecularly imprinted polymers for chemosensing: A mini review. Electrochem. Commun. 2015;50:81-7.

10. Wackerlig J, Schirhagl R. Applications of molecularly imprinted polymer nanoparticles and their advances toward industrial use: A review. Anal. Chem. 2016;88(1):250-61.

11. Turner NW, Jeans CW, Brain KR, Allender CJ, Hlady V, Britt DW. From 3D to 2D: A review of the molecular imprinting of proteins. Biotechnol. Prog. 2006;22:1474-89.

12. Mosbach K, Ramstron O. The emerging technique of molecular imprinting and its future impact on biotechnology. Nat. Biotechnol. 1996;14:163-70.

13. Sullivan MV, Stockburn WJ, Hawes PC, Mercer T, Reddy S, M. Green synthesis as a simple and rapid route to protein modified magnetic nanoparticles for use in the development of a fluorometric molecularly imprinted polymer-based assay for detection of myoglobin. Nanotechnology. 2021;32(9):095502.

14. Sullivan MV, Dennison SR, Archontis G, Hayes JM, Reddy SM. Towards rational design of selective molecularly imprinted polymers (MIPs) for proteins: Computational and experimental studies of acrylamide based polymers for myoglobin. J. Phys. Chem. B. 2019;123:5432-43.

15. Poma A, Guerreiro A, Whitcombe MJ, Piletska EV, Turner APF, Piletsky SA. Solid-phase synthesis of molecular imprinted polymer nanoparticles with a reusable template - "plastic antibodies". Adv. Func. Mat. 2013;23:2821-17.

16. Canfarotta F, Poma A, Guerreiro A, Piletsky SA. Solid-phase synthesis of molecularly imprinted nanoparticles. Nat. Protoc. 2016;11(3):443-55.

17. Subrahmanyam S, Guerreiro A, Poma A, Moczko E, Piletska E, Piletsky S. Optimisation of experimental conditions for the synthesis of high affinity MIP nanoparticles. Eur. Polym. J. 2013;49:100-5.

18. Sullivan MV, Allabush F, Bunka D, Tolley A, Mendes PM, Tucker JHR, et al. Hybrid aptamer-molecularly imprinted polymer (AptaMIP) nanoparticles selective for the antibiotic moxifloxacin. Polym. Chem. 2021;12:4405.

19. Sullivan MV, Clay O, Moazami MP, Watts JK, Turner NW. Hybrid aptamer-molecularly imprinted polymer (aptaMIP) nanoparticles from protein recognition-A trypsin model. Macromol. Biosci. 2021;21(5):e2100002.

20. Martín-Esteban A. Recent molecularly imprinted polymer-based sample preparation techniques in environmental analysis. Trends Environ. Anal. Chem. 2016;9:8-14.

21. Tarannum N, Khatoon S, Dzantiev BB. Perspective and application of molecular imprinting approach for antibiotic detection in food and environmental samples: A critical review. Food Control. 2020;118:107381.

22. Jamieson O, Mecozzi F, Crapnell RD, Battell W, Hudson A, Novakovic K, et al. Approaches to the rational design of molecularly imprinted polymers developed for the selective extraction or detection of antibiotics in environmental and food samples. Phys. Status Solidi. A. 2021;218(13):2100021.

23. Jamieson O, Soares TCC, de Faria BA, Hudson A, Mecozzi F, Rowley-Neale SJ, et al. Screen printed electrode based detection systems for the antibiotic amoxicillin in aqueous samples utilising molecularly imprinted polymers as synthetic receptors. Chemosensors. 2019;8(1):5.

24. Hudson AD, Jamieson O, Crapnell RD, Rurack K, Soares TCC, Mecozzi F, et al. Dual detection of nafcillin using a molecularly imprinted polymer-based platform coupled to thermal and fluorescence read-out. Mat. Adv. 2021;2(15).

25. Hu K, Shi Y, Zhu W, Cai J, Zhao W, Zeng H, et al. Facile synthesis of magnetic sulfonated covalent organic framework composites for simultaneous dispersive solid-phase extraction and determination of β-agonists and fluoroquinolones in food samples. Food Chem. 2021;339:128079.

26. Dai X, Wu Y, Jia Z, Bo C. Preparation of water-compatible magnetic imprinted nanospheres using heptakis (β-cyclodextrin-ionic liquid) as functional monomer for selective recognition of fluoroquinolones in water samples. Microchem. J. 2021;171.

27. Tian H, Liu T, Mu G, Chen F, He M, You S, et al. Rapid and sensitive determination of trace fluoroquinolone antibiotics in milk by molecularly imprinted polymer-coated stainless steel sheet electrospray ionization mass spectrometry. Talanta. 2020;219:121282.

28. Tang Y, Zeng X, Liang J. Surface plasmon resonance: An introduction to a surface spectroscopy technique. J. Chem. Ed. 2010;87(7):742-6.

29. Firdous S, Anwar S, Rafya R. Development of surface plasmon resonance (SPR) biosensors for use in the diagnostics of malignant and infectious diseases. Laser Phys. Lett. 2018;15(6):65602.

30. Cennamo N, D'Agostino G, Pesavento M, Zeni L, . High selectivity and sensitivity sensor based on MIP and SPR in tapered plastic optical fibers for the detection of l-nicotine. Sens. Actuators B, Chem. 2014;191:529-36.

31. Xu X-, Tian X-, Cai L-, Xu Z-, Lei H-, Wang H, et al. Molecularly imprinted polymer based surface plasmon resonance sensors for detection of sudan dyes. Anal. Methods. 2014;6(11):3751-7.

32. Safaryan AHM, Smith AM, Bedwell TS, Piletska EV, Canfarotta F, Piletsky SA. Optimisation of the preservation conditions for molecularly imprinted polymer nanoparticles specific for trypsin. Nanoscale Adv. 2019;1(9):379-3714.

33. Guerreiro AR, Chianella I, Piletska E, Whitcombe MJ, Piletsky SA. Selection of imprinted nanoparticles by affinity chromatography. Biosens. Bioelectron. 2009;24(8):2740-3.

34. Canfarotta F, Cecchini A, Piletsky S. Nano-sized molecularly imprinted polymers as artificial antibodies. In: Polymer Chemistry Series. Chichester, UK: Royal Society of Chemistry; 2018. p. 1-27.

35. Piletsky S, Canfarotta F, Poma A, Bossi AM, Piletsky S. Molecularly imprinted polymers for cell recognition. Trends Biotechnol. 2020;38(4):368-87.

36. Mistry J, Guerreiro A, Moczko E, Piletska E, Karim K, Piletsky SA. Analysis of cooperative interactions in molecularly imprinted polymer nanoparticles. Molecular Imprint. 2016;2(1):55-64.

37. Altintas Z, Guerreiro A, Piletsky SA, Tothill IE. NanoMIP based optical sensor for pharmaceuticals monitoring. Sens. Actuators B, Chem. 2015;213:305-13.

38. Caro N, Bruna T, Guerreiro A, Alvarez-Tejos P, Garretón V, Piletsky S, et al. Florfenicol binding to molecularly imprinted polymer nanoparticles in model and real samples. Nanomaterials. 2020;10(2):306.

39. Kalunke RM, Grasso G, D'Ovidio R, Dragone R, Frazzoli C. Detection of ciprofloxacin residues in cow milk: A novel and rapid optical β-galactosidase-based screening assay. Microchem. J. 2018;136:128-32.

40. Idowu OR, Peggins JO, Cullison R, von Bredow J. Comparative pharmacokinetics of enrofloxacin and ciprofloxacin in lactating dairy cows and beef steers following intravenous administration of enrofloxacin. Res Vet. Sci. 2010;89(2):230-5.

41. Commission regulation (EU) no 914/2010 of 12 oct 2010 amending the annex to regulation (EU) no 37/2010 on pharmacologically active substances and their classification regarding maximum residue limits in foodstuffs of animal origin, as regards the substanc. Chemical Business Newsbase. 2010.

42. Liu C, Tan L, Zhang L, Tian W, Ma L. A review of the distribution of antibiotics in water in different regions of china and current antibiotic degradation pathways. Front. Environ Sci. 2021;9.

43. Tamtam F, Mercier F, Le Bot B, Eurin J, Tuc Dinh Q, Clément M, et al. Occurrence and fate of antibiotics in the seine river in various hydrological conditions. Sci. Total Environ. 2008;393(1):84-95.

44. Hubeny J, Harnisz M, Korzeniewska E, Buta M, Zielinski W, Rolbiecki D, et al. Industrialization as a source of heavy metals and antibiotics which can enhance the antibiotic resistance in wastewater, sewage sludge and river water. PloS One. 2021;16(6):e0252691.

45. Dieguez L, Darwish N, Mir M, Martinez E, Moreno M, Samitier J. Effect of the refractive index of buffer solutions in evanescent optical biosensors. Sens. Lett. 2009;7(5):851-5.

46. Fernandez F, Pinacho DG, Sanchez-Baeza F, Pilar Marco M. Portable surface plasmon resonance immunosensor for the detection of fluoroquinolone antibiotic residues in milk . J. Agric. Food Chem. 2011;59(9):5036-43.

47. Suh YS, Kamruzzaman M, Alam AM, Lee SH, Kim YH, Kim GM, et al. Chemiluminescence determination of moxifloxacin in pharmaceutical and biological samples based on its enhancing effect of the luminol–ferricyanide system using a microfluidic chip. Luminescence J. Biol. Chem. Luminescence. 2013;29(3):248-53.

48. Jiang Z, Li G, Zhang M. A novel sensor based on bifunctional monomer molecularly imprinted film at graphene modified glassy carbon electrode for detecting traces of moxifloxacin. RSC Adv. 2016;6:32915-21.